Journal of Nuclear Materials 377 (2008) 370–377

Contents lists available at ScienceDirect

Journal of Nuclear Materials

journal homepage: www.elsevier.com/locate/jnucmat

The modified relaxation time function: A novel analysis technique for relaxation processes. Application to high-temperature molybdenum internal friction peaks

C.L. Matteo [a,1], O.A. Lambri [b,*,1], G.I. Zelada-Lambri [b], P.A. Sorichetti [a], J.A. García [c]

[a] Departamento de Física, Facultad de Ingeniería, Universidad de Buenos Aires, Avda. Paseo Colón 850, 1063 Buenos Aires, Argentina
[b] Instituto de Física Rosario, Facultad de Ciencias Exactas, Ingeniería y Agrimensura, Laboratorio de Materiales, Escuela de Ing. Eléctrica, Universidad Nacional de Rosario, Avda. Pellegrini 250, (2000) Rosario, Argentina
[c] Departamento de Física Aplicada II, Facultad de Ciencias y Tecnología, Universidad del País Vasco, Apdo. 644, 48080 Bilbao, País Vasco, Spain

ARTICLE INFO

Article history:
Received 12 July 2007
Accepted 19 February 2008

PACS:
61.50.−f
61.72.Lk
61.72.Ji
62.40.+i

ABSTRACT

The modified relaxation time (MRT) function, which is based on a general linear viscoelastic formalism, has several important mathematical properties that greatly simplify the analysis of relaxation processes. In this work, the MRT is applied to the study of the relaxation damping peaks in deformed molybdenum at high temperatures. The dependence of experimental data from these relaxation processes with temperature are adequately described by a Havriliak–Negami (HN) function, and the MRT makes it possible to find a relation between the parameters of the HN function and the activation energy of the process. The analysis reveals that for the relaxation peak appearing at temperatures below 900 K, the physical mechanism is related to a vacancy-diffusion-controlled movement of dislocations. In contrast, when the peak appears at temperatures higher than 900 K, the damping is controlled by a mechanism of diffusion in the low-temperature tail of the peak, and in the high-temperature tail of the peak the creation plus diffusion of vacancies at the dislocation line occurs.

1. Introduction

Molybdenum, a group VI transition metal has a melting point of 2883 K, a high specific heat, and good corrosion and creep resistance. The melting point of molybdenum is exceeded only by tungsten and tantalum, among the useful high-temperature metals. Molybdenum is ductile at room temperature, with a brittle–ductile transition temperature significantly lower than that of tungsten. Molybdenum also has good strength at high temperatures, and is less dense than tungsten and tantalum. In addition, it has a relatively low thermal neutron cross section [1–3]. These qualities make molybdenum attractive for the use in the nuclear industry [4–7]. In fact molybdenum and its alloys are used, for example, in nuclear reactor vessels and other reactor components, detectors in control systems of Tokamak devices and recently they have attracted interest as components for the development of space nuclear reactor power systems [4–6]. Over the past three decades there has been an increasing emphasis on the identification and solution of problems associated with the materials for the construction of a controlled thermonuclear reactor, in particular for those which will be located closest to the plasma, the so-called first-wall region. A broad range of alloys including austenitic stainless steels, ferritic–martensitic steels, refractory metals and titanium alloys have been investigated in extensive international materials testing programmes in order to identify candidate materials for reactor applications [7–9].

The temperature range about 0.3 T_m (T_m being the melting temperature) usually related to the stage V of recovery is particularly interesting in molybdenum; due to the large influence on the mechanical properties of this metal and molybdenum alloys. In fact, neutron irradiation of molybdenum at temperatures <1000 K can result in irradiation embrittlement that is typically characterized by an increase in the ductile to brittle transition temperature, from below room-temperature to values between 873 K and 973 K following irradiation [10]. In the other hand, molybdenum or its alloys as part of nuclear components overcome mechanical stresses and deformation which produce high amount of dislocations. The interaction of dislocation with the defects produced by irradiation is not well known at high temperatures and it can influence the mechanical properties of molybdenum in this high temperature range.

* Corresponding author. Address: Instituto de Física Rosario, Facultad de Ciencias Exactas, Ingeniería y Agrimensura, Laboratorio de Materiales, Escuela de Ing. Eléctrica, Universidad Nacional de Rosario, Avda. Pellegrini 250, (2000) Rosario, Argentina. Tel.: +54 341 480 26 49x125; fax: +54 341 482 17 72/480 26 54.
E-mail address: olambri@fceia.unr.edu.ar (O.A. Lambri).
[1] Member of the Staff of the National Council of Research (CONICET) Argentina.

0022-3115/$ - see front matter © 2008 Elsevier B.V. All rights reserved.
doi:10.1016/j.jnucmat.2008.02.094

Mechanical spectroscopy, also referred to as internal friction, is a non destructive technique and is a fundamental tool for studying the movement of dislocations and their interaction with point defects [11,12]. It involves the simultaneous measurement of the damping or internal friction, Q^{-1}, and the elastic modulus as a function of temperature.

We have reported recently that molybdenum exhibits a damping peak at about 800 K, which is developed in deformed samples after annealing at temperatures above that of the vacancy migration [13,14]. The intensity of the peak depends on previous plastic deformation and the crystal orientation. In fact, the peak is more intense in sample with multiple slip systems. Once the peak is developed the damping was amplitude independent. In addition, the peak was not affected by a bias-stress and the activation energy increases, as the peak temperature increases with annealing treatments. For instance, it increases from 1.6 eV for peak temperature at around 840 K to 2.7 eV for a peak at 1000 K. Besides, the shape of the peak when it appears at temperatures around 1000 K is markedly asymmetrical. Moreover, it has been proposed that the vacancy-dislocation interaction mechanism is controlling this peak [13,14]. Indeed, taking into account the important change in the activation energy, and the change in shape of the damping peak, it would be very interesting to know if the relaxation process is the same for the peak at low and high temperatures. It also would be of great interest to discover whether the activation energy is changing in the reported way, or there exists more than one relaxation process involved in the peak. For instance, one which appears at lower temperatures of about 840 K and another at higher temperatures. An analysis which allows to discern the number of relaxation processes involved in a mechanical spectroscopy peak will be, in general, of high interest for bringing information on the dislocation dynamics in molybdenum and their related energy losses in the temperature interval of 0.3 T_m, in particular.

The modified relaxation time (MRT) function and its applications, derived from a general linear viscoelastic formalism (described in Section 3), is a very useful tool to address the above questions. It must be remarked that the procedure presented in this work, is a novel way to analyse the relaxations peaks in deformed molybdenum at high temperatures, to understand the physical mechanisms involved. The analysis of the results here found for molybdenum could also be applied to other bcc refractory metals as tungsten, niobium or tantalum.

2. Theoretical background

The dynamical response of a linear viscoelastic material is usually described in terms of the complex modulus G^* (or the complex compliance J^*) as functions of the circular frequency ω and temperature T. The complex modulus is generally presented in terms of its real and imaginary parts, that is, $G^* = G' + iG''$, where G' is the storage modulus, G'' is the loss modulus, and i is the imaginary unit [15].

It is well known that for each temperature T, G^* can be completely determined given $\Pi(T,\ln\tau)$, the non-normalized distribution function of relaxation times τ, together with the unrelaxed modulus $G_u(T)$, that is, the limit of $G^*(T,\omega)$ for $\omega \to \infty$

$$G^*(T,\omega) = G_u(T) - \int_{-\infty}^{\infty} \Pi(T,\ln\tau)\frac{d(\ln\tau)}{1+i\omega\tau} \tag{1}$$

The non-normalized distribution function Π represents the contribution to relaxation modulus of the relaxation times within the interval $(\ln\tau, \ln\tau + d\ln\tau)$. The relaxed modulus G_r is calculated from Eq. (1) as

$$G_r(T) = G^*(T,\omega=0) = G_u(T) - \int_{-\infty}^{\infty} \Pi(T,\ln\tau)d(\ln\tau) \tag{2}$$

The integral in Eq. (2) is usually called the relaxation magnitude $\delta G(T)$, which it is given by

$$\delta G(T) = \int_{-\infty}^{\infty} \Pi(T,\ln\tau)d(\ln\tau) = G_u(T) - G_r(T) \tag{3}$$

It is useful to define a dimensionless magnitude Δ, usually called the relaxation strength, in terms of the characteristic parameters of the modulus

$$\Delta(T) = \frac{\delta G(T)}{G_r(T)} \tag{4}$$

Also, a dimensionless distribution function of relaxation times may be defined by

$$\Psi(T,\ln\tau) = \frac{\Pi(T,\ln\tau)}{G_r} \tag{5}$$

Finally, the internal friction (also called loss tangent) is defined as the quotient between the imaginary and real part of the complex modulus

$$Q^{-1}(T,\omega) = \frac{G''(T,\omega)}{G'(T,\omega)} = \frac{G''(T,\omega)/G_r(T)}{G'(T,\omega)/G_r(T)} \tag{6}$$

In terms of the dimensionless distribution function, Eq. (5), Q^{-1} may be written as

$$Q^{-1}(T,\omega) = \frac{\int_{-\infty}^{\infty} \Psi(T,\ln\tau)\frac{\omega\tau}{1+(\omega\tau)^2}d(\ln\tau)}{1+\int_{-\infty}^{\infty} \Psi(T,\ln\tau)\frac{(\omega\tau)^2}{1+(\omega\tau)^2}d(\ln\tau)} \tag{7}$$

Taking into account Eqs. (3)–(5) it is easy to see that the function Ψ is also a non-normalized distribution function, since

$$\int_{-\infty}^{\infty} \Psi(T,\ln\tau)d(\ln\tau) = \Delta(T) \tag{8}$$

It should be pointed out that the internal friction obtained from the complex modulus in Eq. (6) will take the same values, at the same temperature and frequency, if it is derived from the complex compliance, although the distribution function involved will be a different one.

2.1. The Debye process

For the Debye process, a distribution function characterized by an unique relaxation time, $\tau_D(T)$, is often employed to describe relaxation processes; due to its conceptual simplicity. In this case

$$\Psi(T,\ln\tau) = \Delta(T)\delta(\ln\tau - \ln\tau_D(T)) \tag{9}$$

where δ is the Dirac function. Therefore, Eq. (6) can be written, see reference [12]

$$Q^{-1}(T,\omega) = \frac{\Delta(T)}{\sqrt{1+\Delta(T)}}\frac{\omega\tau_t(T)}{1+(\omega\tau_t(T))^2} \tag{10}$$

with

$$\tau_t(T) = \sqrt{1+\Delta(T)}\tau_D(T) \tag{11}$$

On the other hand, if experimental data cannot be represented by a single Debye process, different approaches have been developed for the analysis [12,15]. The conventional tools for the analysis of complex relaxation processes, usually based on distribution functions of Debye relaxation times, are not easily applicable to experimental results, since the problem is mathematically 'ill-posed'. In consequence, ad-hoc procedures for the fitting of measured data are usually employed, such as those based on Thikonov regularization [12,15]. This work presents a different, novel way to represent the

internal friction and, therefore, re-analyze its characteristic parameters.

3. The modified relaxation time (MRT) function

The internal friction represented by Eq. (7) can be written in a different way. In previous works [16,17] it has been rigorously demonstrated that the Q^{-1} can be expressed in terms of two functions, $\Lambda(T)$ and $\tau_t(T,\omega)$ as follows:

$$Q^{-1}(T,\omega) = \Lambda(T)\frac{\omega\tau_t(T,\omega)}{1+[\omega\tau_t(T,\omega)]^2} \tag{12}$$

where $\Lambda(T)$ is the envelope function and $\tau_t(T,\omega)$ is the *modified relaxation time function (MRT function)*, indicated in Refs. [16,17] as the integrated distribution function. As shown in these references, the existence of these functions is guaranteed by the existence of the tangent distribution function (TDF) $\Phi(T,\ln\tau)$ which allows the internal friction to be expressed as a single integral, that is

$$Q^{-1}(T,\omega) = \int_{-\infty}^{\infty}\Phi(T,\ln\tau)\frac{\omega\tau}{1+(\omega\tau)^2}\mathrm{d}(\ln\tau) \tag{13}$$

The TDF can be derived from Eq. (6), as it is demonstrated in the Appendix of Ref. [16], as

$$\Phi(T,\ln\tau) = \lim_{a\to 0^+}\frac{1}{\pi}\left[Q^{-1}(T,a+i/\tau) - Q^{-1}(T,-a+i/\tau)\right] \tag{14}$$

leading to

$$\Phi(T,\ln\tau) = \frac{\Psi(T,\ln\tau)\left[1+\int_{-\infty}^{\infty}\frac{\Psi(T,\ln u)}{1+(\tau/u)}\mathrm{d}(\ln u)\right]}{\frac{\pi^2}{4}\Psi^2(T,\ln\tau)+\left[1+\int_{-\infty}^{\infty}\frac{\Psi(T,\ln u)}{1-(\tau/u)^2}\mathrm{d}(\ln u)\right]^2} \tag{15}$$

This theoretical result has many important consequences (see, for example Ref. [14]) and one of them is to validate Eq. (12). In fact, for distribution functions with a single peak, it is easy to see that the envelope function is the normalization of the TDF, that is

$$\Lambda(T) = \int_{-\infty}^{\infty}\Phi(T,\ln\tau)\mathrm{d}(\ln\tau) \tag{16}$$

In a measurement of internal friction as a function of frequency, at constant temperature, which usually gives a single-peaked function, $\Lambda(T)$ represents simply the double of the peak value, since the loss tangent takes its maximum value at the frequency where $\omega\tau_t(T,\omega) = 1$. On the other hand, in a measurement of internal friction as a function of temperature at constant frequency, $\Lambda(T)$ represents the envelope of the family of Q^{-1} vs. T curves, since $Q^{-1}(T,\omega) \leqslant \Lambda(T)/2$ for all ω.

3.1. Analysis of thermally activated processes using the MRT function

The MRT function can be used to analyse the relaxation distribution involved in thermally activated processes. Usually, the shift of the peak temperature in the internal friction peaks with frequency has been widely used to determine the activation energy in this kind of processes [11,12]. In fact, assuming that the characteristic relaxation time of the present distribution function depends on temperature as

$$\tau(T) = \tau_0\exp(H/kT) \tag{17}$$

and at the peak temperature is such that $\omega\tau(T) = 1$, the mean activation energy, H, can be obtained from the slope of the straight line fitted to the data pairs frequency and temperature, evaluated at the maximum in the Q^{-1} peak ($\ln(1/\omega_p, 1/T_p)$) [11,12]. This procedure is the so called Arrhenius plot [11,12]. In Eq. (17) k is the Boltzmann constant and τ_0 is the mean pre-exponential factor. However, this procedure does not give any information about the distribution function that describes the internal friction peak, and in particular, whether there are or not several closely spaced relaxation times around the principal one.

In order to show the advantages of the MRT formalism the Havriliak–Negami (HN) parametrical expression for dynamical modulus will be used. This is defined by [18,19]

$$G^*(T,\omega) = G_u(T) - \frac{\delta G(T)}{[1+(i\omega\tau^*(T))^{\alpha(T)}]^{\beta(T)}} \tag{18}$$

This function has been used to generate different Q^{-1} vs. T curves, for several frequencies and relaxation strength values. The values of α and β are the characteristic parameters of HN function, while relaxation time $\tau^*(T)$ has been simulated by using Eq. (17) for different values of H. α and β are phenomenological parameters that described the symmetrical and asymmetrical broadening of the peak, respectively. In fact, these behaviours are related to the loss modulus, which could lead to slightly differences in Q^{-1}. For simplicity, α, β and Δ will be considered independent of temperature in the following cases. In addition, it is convenient to mention that α and β are introduced as phenomenological parameters to describe the broadening of the relaxation peak (in comparison to the Debye model) and in consequence do not have, up to the present, a clear physical interpretation.

Fig. 1(a)–(c) shows a few typical cases of internal friction peaks and the corresponding MRT functions vs. temperature curves. In all cases it is evident that the MRT functions are independent of the relaxation strength. The MRT functions show a linear behaviour on both sides of the peak, but the slopes of the linear sections on each side of the peak have a different dependence on the activation energy and on the parameters of the HN function.

It should be highlighted that on the high-temperature side, the slope of the MRT function, S_H is found to be very close to

$$S_H = \alpha H \tag{19}$$

and therefore it is independent of the value of β. In addition, on the low-temperature side, the slope S_L is found to be nearly equal to

$$S_L = \alpha\beta H \tag{20}$$

Eqs. (19) and (20) have been verified through extensive numerical computations spanning all the physically meaningful range of the variables α, β, Δ and H. This remarkable, novel result highlights the usefulness of the MRT formalism for the analysis of experimental data of relaxation processes.

When β is different from 1, there is a change in the slope of the MRT function, and the quotient between S_L and S_H is directly the value of the parameter β. Moreover, both slopes are proportional to the activation energy H. In the Debye case, that is, when $\alpha = 1$ and $\beta = 1$, the function is a straight line and its slope is directly the value of H, as it could be expected.

It should be emphasized that in the novel procedure for the analysis of relaxation processes, described above, the MRT function depends only on the dimensionless distribution function, Eq. (5), and in consequence it is independent of the relaxation strength and the relaxed modulus.

Moreover, for processes described by the Havriliak–Negami function, the slope of the MRT, as a function of temperature at a given frequency, is proportional to the shape parameters, α and β, and the activation energy H. Therefore, the graphical representation of the MRT makes much easier identify the characteristic parameters related to the shape and symmetry of the distribution function of relaxation times involved in the process.

4. Experimental

4.1. Samples

The single crystals used in this work were prepared from zone refined single-crystal rods of molybdenum in A.E.R.E., Harwell. The high purity molybdenum crystals were prepared from a single

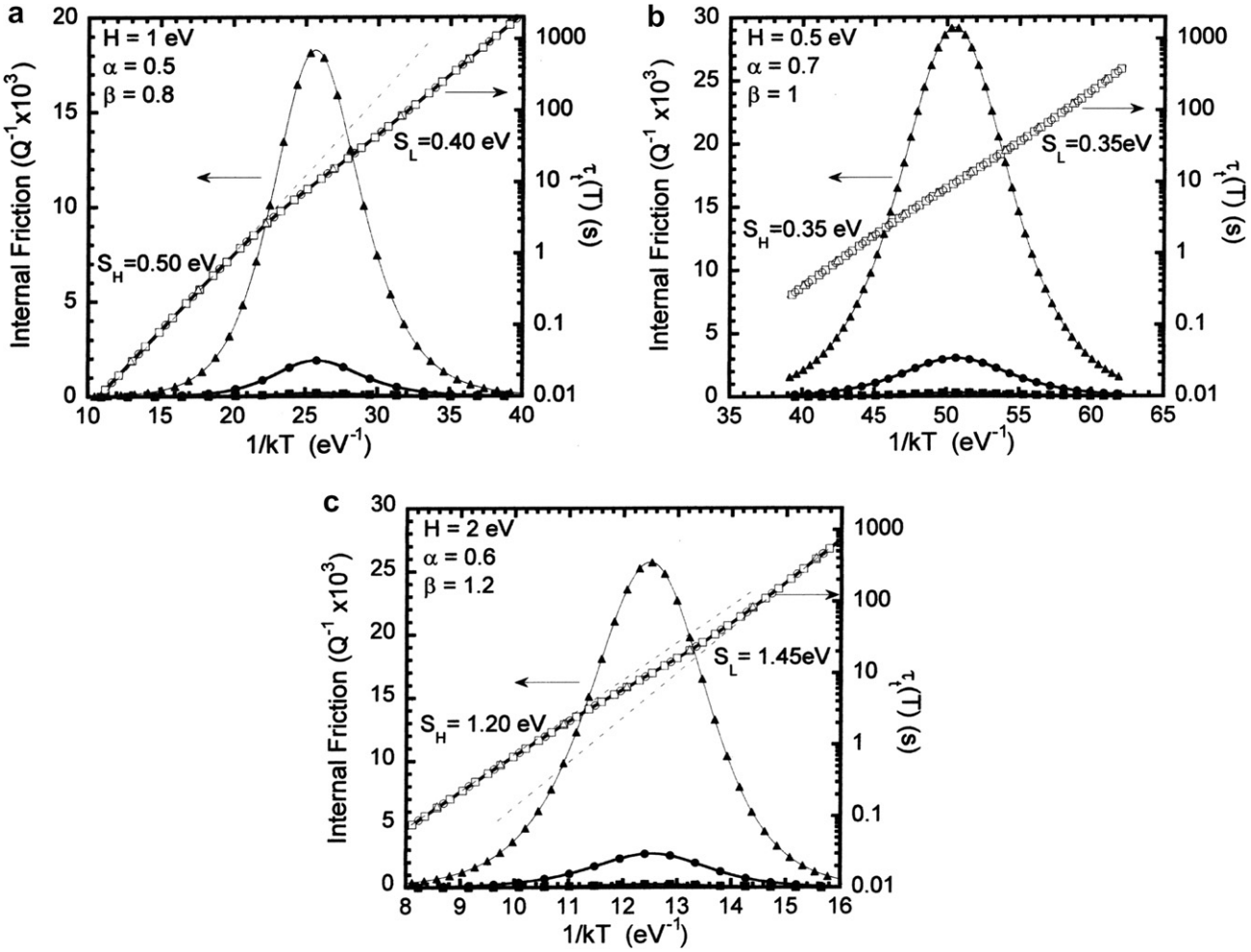

Fig. 1. Internal friction peaks (full symbols) and MRT functions (empty symbols) for the case of a HN function, with different relaxation strengths. Squares: $\Delta = 0.001$, circles: $\Delta = 0.01$, triangles: $\Delta = 0.1$. (a) Case $\beta < 1$. (b) Case $\beta = 1$. (c) Case $\beta > 1$.

bach of 'Amax Specialty Metals Corporation' low carbon 3/8" diameter rods. The specifications of this starting material were: C 0.004%, O_2 0.0004%, H_2 0.0001%, N_2 0.0001%, Fe 0.002%, Ni 0,001% and Si 0.002%. Samples with different orientations were prepared from 6-pass zone refined molybdenum, which was decarburized at 1873 K for 48 h and annealed at 2073 K for 3 h in a vacuum better than 10^{-7} Torr. The total final content of (C, O, H, N, Fe, Ni, Si, W) was under 10 at. ppm, the main residual impurity, being tungsten.

The residual resistivity, RR, of the samples was about 8000. RR is calculated from the ratio between the electrical resistivity value measured at room temperature and the value of the electrical resistivity measured at liquid helium temperatures. Samples with the ⟨1 1 0⟩ and ⟨1 4 9⟩ crystallographic tensile axis were used to favour deformation by multiple and single slip, respectively. The samples were sheets of 20 mm length, 0.2 mm thickness and 2 mm width. The samples were annealed at 1973 K during 24 h and at 2273 K during three hours, both under high vacuum. Subsequently they were deformed in tensile at a constant speed of 0.03 cm/min, followed by torsion at room temperature. The characteristics of the samples studied in this work are shown in Table 1. Single crystals, after plastic deformation and damping tests, were checked by means of Laue photographs and metallographical studies. Laue and light microscopy results indicated that the single-crystalline state was not changed by the plastic deformation or annealing to the work temperatures [14].

Table 1
Sample descriptions

Sample type	Orientation	Elongation (%)	Torsion (%)
I	⟨1 1 0⟩	5	1
II	⟨1 1 0⟩	3	1
III	⟨1 4 9⟩	5	1

4.2. Mechanical spectroscopy measurements

Damping and natural frequency were measured in an inverted torsion pendulum, under a vacuum of about 10^{-7} Torr. The equipment can also apply a bias stress or 'in situ' deformation. The maximum strain on the surface of the sample was 5×10^{-5}. The maximum strain refers to the maximum value which is produced in a rectangular bar under torsion for a given torsional angle. Indeed a rectangular bar under torsion exhibits a non uniform distribution on strain depending of the place on its rectangular section. The iso-deformation zones are hyperbolae with a center shifted from the center of mass of the rectangular section towards a vertex. The maximum strain region is over the boundary parallel to the larger edge of the rectangular section [20]. This non homogeneity in the field of strain (or stresses) during the torsional vibrations does not produce effects on the measured damping since it is independent of the amplitude of oscillation once the peak has developed [14,20].

The measurement frequency was around 1 Hz except for the determination of the frequency dependence of the peak temperature. The heating and cooling rates employed in the test were of 1 K/min. A heating ramp and its corresponding cooling run will be called hereafter a thermal cycle. There was no hold time between the heating and the cooling ramps once the maximum temperature had been achieved, i.e. once that the maximum temperature is achieved during the heating ramp, the cooling run starts without annealing time at the maximum temperature.

During the thermal cycles, Q^{-1}, was calculated from the slope of the straight line which results from the least squares fitting of the natural logarithm of all the decaying amplitudes (areas) versus time [14]. For all these measurements the same initial and end values of the decaying amplitudes were used eliminating any possible distortion due to amplitude-dependent damping effects [20].

The longest time employed for recording the decay during the heating runs was shorter than 60 s. In fact, the recording time was about 10 s in order to hold the ratio between the area of the nth decaying oscillation, A_n, and the initial area of the starting decaying oscillation, A_0, at Q^{-1} values of about 0.01. Consequently each measured damping point has an accuracy in temperature better than 1 K. The temperature indicated in the Figures in the next Section corresponds to a recorded value corresponding to the sample. The thermocouple is located in contact with the fixed grip of the pendulum, machined in stainless steel, at 1 mm of the sample. Previous calibrations of this lecture with respect to two other thermocouples in contact with the samples, located at around 10 mm and 20 mm from the other one, give a good agreement between all lectures with a scattering less than 0.3 K for the heating rate employed in the present work.

5. Results

Fig. 2 shows the damping spectra of a type III sample, in order to show the general characteristics of the raw measured damping experiments. During the first heating up to 973 K, after the room temperature deformation, the sample showed an increasing background with temperature (see curve a, heating in Fig. 2). Nevertheless, on cooling a well developed internal friction peak at around 700 K was present (curve a, cooling). Successive thermal cycles up to 973 K lead to the stabilisation of the peak temperature and peak height, as seen in spectrum b of the same figure. However, thermal cycles performed after annealing above 1200 K, lead to a shift in the peak towards higher temperatures (curve c). In addition, it can be also inferred that the asymmetry of the peak increases.

Samples of ⟨1 1 0⟩ orientation (types I and II, in Table 1) present similar behavior. Fig. 3 shows the change in peak position (spectra D and E in the figure) for a deformed sample of type I after annealing at two different temperatures 1050 K and 1230 K, respectively. In all the samples, the activation energy for the relaxation peak increases as the temperature of the peak increases. For peak temperature at around 840 K the measured activation energy was 1.6 eV and 2.7 eV for a peak at 1000 K. Values between 1.6 eV and 2.7 eV were obtained for intermediate temperatures of the relaxation. A detailed experimental study of the behaviour of the mechanical spectra and activation energies as a function of annealing temperature and strain in the different kinds of samples was already reported in Refs. [13,14].

Fig. 4 shows the damping peaks for the samples of types I and II, after background subtraction. Background subtraction was performed by means of cubic polynomials [21]. Curves A, B and C correspond to damping peaks obtained from a stabilised damping spectrum measured in a type II sample at a natural frequency of about 0.2 Hz, for thermal cycles with maximum temperatures of 1040 K, 1100 K and 1155 K, respectively; see reference [14]. The resulting peak temperatures were around 900 K, 940 K and 960 K, respectively. Peaks labeled D and E correspond to the

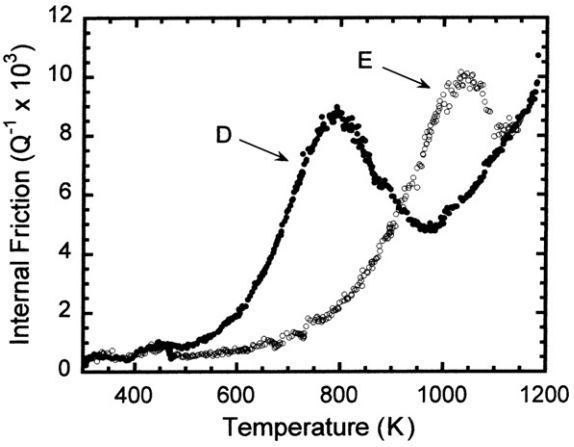

Fig. 3. Damping as a function of temperature for a molybdenum sample of type I (⟨1 1 0⟩ orientation), after thermal cycles up to 1050 K (spectrum D) and 1230 K (spectrum E).

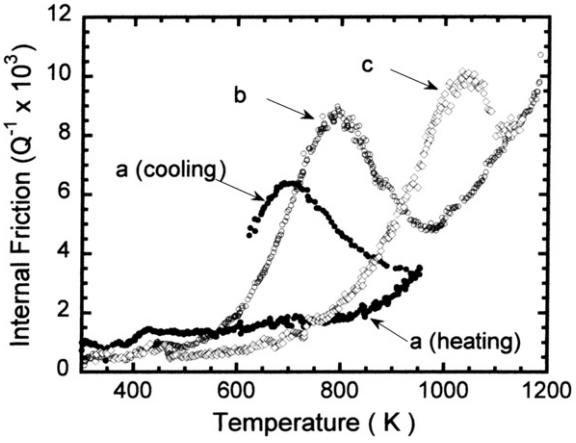

Fig. 2. Damping as a function of temperature for a molybdenum sample of type III (⟨1 4 9⟩ orientation) during different heating and cooling runs.

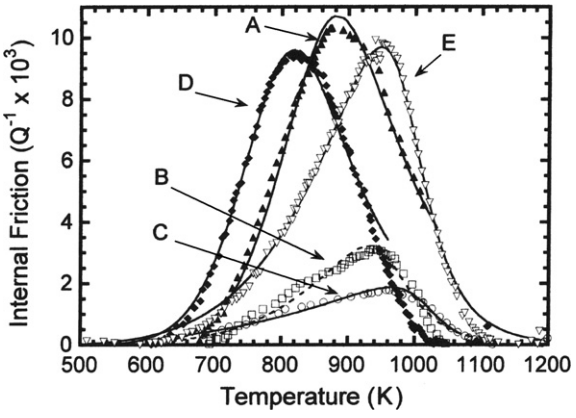

Fig. 4. Internal friction peaks after background subtraction (symbols) for the molybdenum samples of ⟨1 1 0⟩ orientation (types I and II). Full lines represent the numerical fitted peaks.

sample of type I shown in Fig. 3 after background subtraction and stabilization during thermal cycles up to temperatures of 1050 K and 1230 K, respectively. In this figure we have summarized the relaxation peaks measured in ⟨1 1 0⟩ samples in order to study the response of the MRT formalism.

The calculated curves of the logarithm of the MRT as a function of $1/kT$ (i.e. $\ln(\tau_t(\omega,T))$ vs. $1/kT$), corresponding to peaks in Fig. 4 are given in Fig. 5. In this figure we have plotted part of the calculated points with the MRT function for clarity. Curve corresponding to the peak B has not been included for clarity, but it has a similar behaviour to the plotted curves, E and C. Vertical arrows in the figure indicate the temperature T_p corresponding to the maximum value of damping (Q_p^{-1}). S_H and S_L indicate the slope at high-temperature and low-temperature of the fitted straight lines (full lines), as defined in Eqs. (19) and (20).

It has to be remarked that for curves A and D two linear zones with the same slope were found in the MRT plot, in spite of the scatter of the calculated data. For temperatures far from the peak temperature the linearity is lost, as it could be expected due to the error introduced in the data by the background subtraction procedure. For this kind of behaviour of the MRT, it was shown in Section 3.1 that the distribution functions of relaxation times should be symmetrical. In contrast, for spectra B (not shown in the figure), C and E two clearly linear zones with different slopes were found. The behaviour of the MRT function indicates that these relaxation peaks should be asymmetrical, in agreement with the experimental results. Therefore, for these peaks it can be proposed that at least two overlapped relaxations occur; where each one can be described through its correspondingly distribution function of relaxation times. It should be emphasized that in the calculation of the MRT curves plotted in Fig. 5, no assumptions or restrictions were made about the shape of the distribution function of relaxation times. The fact that these MRT functions appear to be linear on both sides of each peak temperature, indicates that a HN model may be applied, as described in Section 3, with the parameters α, β and Δ being approximately constant with temperature, at least in the temperature range encompassed by the internal friction peak.

From the slopes of the straight segments fitted to the ln (MRT) vs. $1/kT$ curves (full lines in Fig. 5); the parameters of the HN distribution function can be obtained by means of Eqs. (19) and (20), as it was shown in Section 3.1. Table 2 gives the calculated parameters for the HN function together with relevant experimental information related to each damping peak.

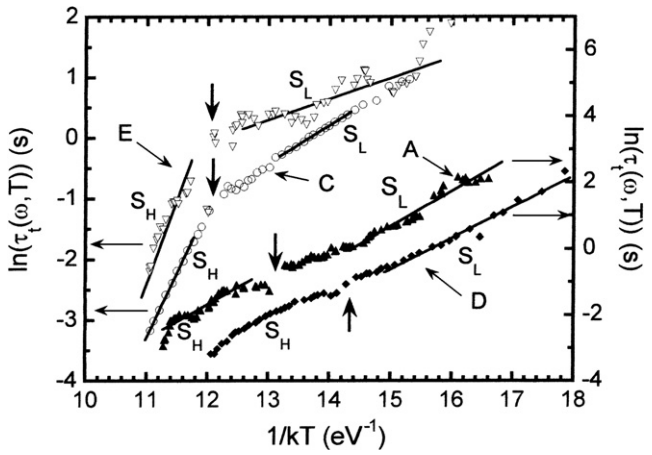

Fig. 5. Natural logarithm of MRT as a function of $1/kT$ for the peaks plotted in Fig. 4, corresponding to samples of ⟨1 1 0⟩ type. Vertical arrows indicate the position of the peaks on the $1/kT$ axis. Full lines indicate the linear zones in the MRT graphs, see text. Also, S_H and S_L are defined in the text (Section 3).

Table 2
Experimental and theoretical results for the studied relaxation peaks

Peak name/ sample type	AT (K)	T_p (K)	$Q_p^{-1} \times 10^3$	H (eV)	α	β	Calculated	
							T_p (K)	$Q_p^{-1} \times 10^3$
A/II	1040	880	10.3	1.8	0.58	→1	880	10.7
B/II	1100	940	3.0	2.0	→1	0.3	935	3.2
C/II	1155	960	1.7	2.75	→1	0.12	960	1.9
D/I	1040	817	9.5	1.6	0.6	→1	817	9.6
E/I	1230	949	9.8	2.1	→1	0.25	949	9.8
b/III	973	780	6.5	1.6	0.7	0.7	780	6.5
c/III	1230	1018	4.8	2.7	→1	0.3	1018	4.8

AT: annealing temperature, Q_p^{-1}: damping value at the maximum, T_p: temperature for the Q_p^{-1}. α and β: parameters of the Havriliak–Negami function. H: activation energy, taken from Ref. [14].

The damping peaks calculated theoretically by means of Eqs. (6) and (18) using the fitted parameters of the HN function are also shown in Fig. 4 by means of full lines. The activation energy for the calculation of Eq. (18), using Eq. (17), is the value that we obtained previously from the usual Arrhenius procedure, see reference [14] and Table 2. The use of this value of the activation energy for the HN function is supported by the fact that, even if there is a distribution of relaxation times, the experimentally measured $\tau(T)$ (Eq. (17)) corresponds to the mean value of the distribution function such that

$$\tau(T) = \lim_{M\to\infty} \int_{-M}^{M} \tau(T, \ln\omega) \mathrm{d}\ln\omega \tag{21}$$

The peak temperature and peak height for the calculated relaxations are also listed in Table 2.

As it can be seen from Fig. 4, the agreement between the experimental and calculated peaks is good, indicating that the calculated parameters of the HN function (α and β) are appropriate for describing the relaxation peaks in molybdenum at temperatures of about 0.3 T_m. Therefore, from the study of the behaviour of α and β parameters as a function of temperature valuable information can be obtained about the physical process controlling the relaxation peaks.

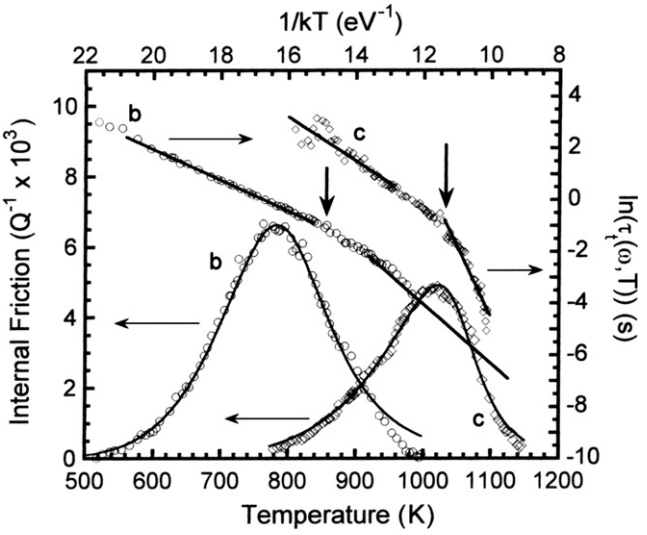

Fig. 6. Damping peaks after the background subtraction (lower and left axis) for a sample of type III and their corresponding ln(MRT) vs. $1/kT$ (upper and right axis). Vertical arrows have the same meaning as in Fig. 5. Full lines over the peaks represent the numerical results. Full lines over the MRT graphs indicate the linear zones, see text.

Fig. 6, shows the damping peaks for the type III ⟨149⟩ sample presented in Fig. 2 after background subtraction. Also shown in the same figure are the logarithms of the MRT function for both peaks, upper and right axis. Vertical arrows in the Figure indicate the peak temperature for $1/kT$ axis. In this figure we have also plotted part of the calculated points with the MRT function for clarity.

MRT results indicate that the peak at lower temperature is slightly asymmetrical ($\beta = 0.7$) and the peak at higher temperature is stronger asymmetrical ($\beta = 0.3$). This result can be also inferred from the behavior of the straight lines in the logarithm of the MRT curves. In addition, the re-constructed theoretically damping peaks are also plotted by means of full lines, achieving a good agreement between the theory and experimental data. Experimental points plotted in the figure for the damping peaks were 1 of each 3 ones, for clarity.

6. Discussion

Fig. 7 shows the calculated α and β parameters as a function of temperature for samples of I and II type (circles). It is interesting to note that the peaks A and D were mainly symmetrical ($\beta \to 1$) but broader ($\alpha < 1$) than a Debye peak, in agreement with previous works [13,14], where the half-width of the peaks was evaluated by means of the traditional analysis [11,12]. Indeed, the peaks which appear at temperatures well below 900 K, obtained during annealing up to temperatures smaller than about 1100 K, can be described by a symmetrical distribution function of relaxation times, with an average activation energy represented by the value obtained from the Arrhenius plot. In addition, a good agreement was also found for relaxation peaks during thermal cycles up to 973 K in type I samples with a Q_p^{-1} of about 20×10^{-3}. This indicates that the same physical mechanism occurs when the sample is heated below 1100 K.

For peaks B, C and E (with $T_p > 900$ K), which correspond to samples heated above 1100 K, the α and β parameters are: $\beta < 1$ and $\alpha \to 1$, revealing that the peaks are asymmetrically broadened. This means that there is an overlapping of relaxation processes leading to an asymmetrical broadening of the peak. Remember that α and β are the phenomenological parameters that described the symmetrical and asymmetrical broadening of the peak, respectively and that for $\alpha \to 1$ does not lead to a Debye width when $\beta \neq 1$.

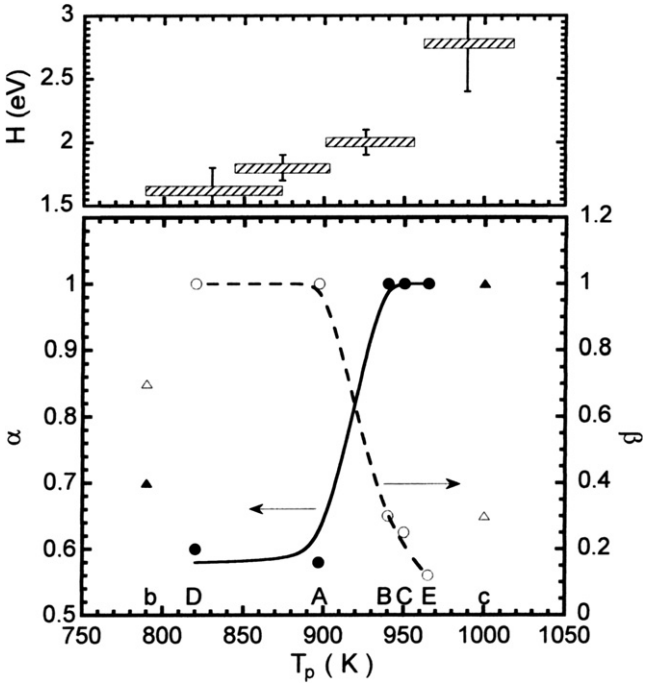

Fig. 7. Lower plot: Parameters of the HN function as a function of peak temperature, T_p. Circles: samples of types I and II. Triangles: Samples of type III. Labels in the Figure correspond to data in Table 2. Upper plot: Activation energy as a function of T_p calculated from the Arrhenius plot, taken from Ref. [14].

Moreover, C and E peaks which have close peak temperature (≈950 K) and very different relaxation intensities (by a factor about 5) exhibit similar α and β parameters, indicating an effect only on the relaxation strength, in agreement with the explanation given above for the peak at lower temperature. However, the physical mechanism controlling these asymmetrical peaks at higher temperatures is different to the physical mechanism giving rise to the symmetrical peaks found at lower temperatures. This point will be discussed more in detail in the next paragraphs.

Triangles in Fig. 7 correspond to the sample of III type. Despite they are not fitting well in the calculated curves for the ⟨110⟩ samples, the ⟨149⟩ sample shows a similar behaviour. In fact, β decreases as the peak temperature increases and α increases as the T_p increases, reaching a value close to 1 at elevated temperatures. Therefore, for the ⟨149⟩ samples even in the lower temperature peak the MRT method is indicating that at least two processes are relaxing simultaneously. This is a remarkable result since in the ⟨149⟩ samples peaks were unstable; i.e. they changed their peak temperature and intensity during the thermal cycles [13,14] which made very tedious the calculus of the activation energy at lower temperatures for the ⟨149⟩ samples.

The discrepancy between the values found for the peak at lower temperatures for samples ⟨110⟩ and ⟨149⟩ are related to a different dislocation arrangement in each sample and to the problem of non-stabilization of the microstructure in the ⟨149⟩ sample during the thermal cycles up to temperatures lower than 1230 K, see references [13,14]. For the peak at higher temperature, the α and β values calculated for the ⟨149⟩ sample are more alike the obtained in the ⟨110⟩ samples, being this difference controlled by the different dislocation arrangement. In fact, ⟨110⟩ exhibited a larger quantity of slip systems than ⟨149⟩ samples, which is oriented for single slip. Consequently, as it was pointed out above, we will discuss in more detail the results for the ⟨110⟩ samples; in the following paragraphs.

The change in the α and β parameters as a function of peak temperature calculated for ⟨110⟩ samples, seen in Fig. 7, reveals that in a temperature interval of less than 40 K, the parameter α changes by almost 100% and parameter β changes about one order of magnitude. Consequently, it can be established that there exist two relaxation processes in molybdenum in the temperature range of 0.3 T_m. The first relaxation process is related to the symmetrical peak which appears between 820 K and 900 K, and the other to the asymmetrical peak which appears at higher temperatures, from about 950 K. The low-temperature peak is developed in deformed samples after annealing at temperatures above that of vacancy diffusion and the higher temperature peak appears at temperatures near to 0.3 T_m [13,14].

In molybdenum the reported values [22,23] for the migration energy of vacancies range between 1.35 eV ⩽ Hvm ⩽ 1.60 eV. Taking into account the measured activation energy of 1.6 eV for the lower temperature peak, we can relate this peak to the dragging of vacancies by the dislocation line controlled by a diffusion mechanism. In contrast, when the peak appears at higher temperature, results show that it is controlled by another mechanism. This mechanism is consistent with the creation and diffusion of vacancies in the dislocation line, in agreement with the activation energy we measure for the high-temperature peak (2.7 eV). In fact, the self diffusion energy for vacancies, Hsd can be written as the sum of the formation energy (3.0 eV ⩽ Hvf ⩽ 3.2 eV) [23,24] and migration energy (1.35 eV ⩽ Hvm ⩽ 1.60 eV). When the self diffusion is pro-

duced in the core of the dislocation line the value is reduced by a factor between 0.6 and 0.8. This results in activation energies in the range 2.6–2.9 eV, very close to the 2.7 eV measured for the high-temperature peak.

It is interesting to note that for the peaks at high temperatures (about 950 K) the activation energy obtained from the Arrhenius plot (see upper plot in Fig. 7) does not yet reveal clearly the appearance of the mechanism of vacancy creation, because in the calculation of the activation energy its value is averaged over a range of about 50 K and the contribution of the diffusive part could mask the appearance of the vacancy creation mechanism.

The appearance of the mechanism of vacancy creation can explain also the strong asymmetry of the peak at higher temperatures. During the heating run, within the temperature interval corresponding to the low temperature tail of this peak, the relaxation process is controlled mainly by a diffusion mechanism. In contrast, for the high-temperature tail of the peak, the new vacancies produced by the dislocation movement enhance the mobility of dislocations, giving rise to a larger decrease in the damping values as the temperature is increased. The enhancement of the movement of dislocation due to vacancy creation has been recently reported for magnesium in the range of 0.3 T_m [25].

Indeed, it should be highlighted, that the possibility of discriminating the physical mechanisms (and their related parameters) depending on the temperature interval, could be very useful, e.g., for describing the anelastic creep behaviour both from a rheological or phenomenological point of view; in molybdenum and its alloys.

7. Conclusions

A novel method has been presented to analyze relaxation processes in terms of the modified relaxation time (MRT) function. The MRT depends only on the dimensionless distribution function, Eq. (5), and in consequence is independent of the relaxation strength and the relaxed modulus. Numerical examples were presented in this work of the analysis of thermally activated processes described by Havriliak–Negami function.

It should be highlighted that the slope of the MRT as a function of temperature, when applied to processes described by the HN function, is shown to be proportional both to the shape parameters, α and β and also to the activation energy, H.

The MRT procedure was applied to a HN fit of experimental results of mechanical spectroscopy in high purity single-crystalline molybdenum, with excellent results. The analysis indicates that the distribution of relaxation times is symmetrical for peaks below 900 K and asymmetrical at higher temperatures.

The values of α and β parameters calculated as a function of temperature reveal that the lower temperature relaxation mechanism is different to the higher temperature one. The lower temperature relaxation was related to vacancy-diffusion-controlled movement of dislocations. The higher temperature peak was related to a process controlled by diffusion in the low-temperature tail of the peak, and by the creation plus diffusion of vacancies at the dislocation line, in the high-temperature tail of the peak.

The use of the MRT for the discrimination of the physical mechanisms (and their related parameters) according to the different temperature ranges, could also be very useful to describe the results of other tests of technological interest, as in the case of anelastic creep.

Acknowledgements

We acknowledge to Professor J.N. Lomer for the interest in the present work and for the single crystal samples. This work was partially supported by the Collaboration Agreement between the Universidad del País Vasco and the Universidad Nacional de Rosario Res. CS.788/88-1792/2003, UPV224.310-14553/02 and Res. C.S. 3469/2007, the CONICET-PIP No. 5665 and 6465 and the PID-UNR 2005–2007.

References

[1] S. Nemat-Nasser, W. Guo, M. Liu, Scripta Mater. 40 (1999) 859.
[2] E.R. Braithwaite, J. Haber, Molybdenum: An Outline of Its Chemistry and Uses, Elsevier, New York, 1994.
[3] Y. Ishima, K. Kakiuchi, T. Furuya, H. Kurishita, J. Nucl. Mater. 307–311 (2002) 1369.
[4] M.S. El-Genk, J.M. Tournier, J. Nucl. Mater. 340 (2005) 93.
[5] B.V. Cockeram, J.L. Hollenbeck, L.L. Snead, J. Nucl. Mater. 324 (2004) 77.
[6] A.A. Ivanov, M.V. Kollegov, V.V. Kolmogorov, E.A. Kuper, A.S. Medveko, A.N. Shukaev, in: Eighth International Conference on Accelerator and Large Experimental Physics Control Systems, San José, California, TUAP017, 2001.
[7] D.J. Mazey, C.A. English, J. Less Common Metals 100 (1984) 385.
[8] R.C. Rau, J. Moteff, R.L. Ladd, J. Nucl. Mater. 40 (1971) 233.
[9] V. Chakin, V. Kazakov, J. Nucl. Mater. 233–237 (1996) 570.
[10] B.V. Cockeram, J.L. Hollenbeck, L.L. Snead, J. Nucl. Mater. 336 (2005) 299.
[11] R. Schaller, G. Fantozzi, G. Gremaud (Eds.), Mechanical Spectroscopy 2001, Trans. Tech. Publications, Uetikon-Zuerich, Switzerland, 2001.
[12] A.S. Nowick, B.S. Berry, Anelastic Relaxation in Crystalline Solids, Academic, New York, 1972.
[13] O.A. Lambri, G.I. Zelada-Lambri, L.M. Salvatierra, J.A. García, J.N. Lomer, Mater. Sci. Eng. A 370 (2004) 222.
[14] G.I. Zelada-Lambri, O.A. Lambri, J.A. García, J. Nucl. Mater. 353 (2006) 127.
[15] N.W. Tschoegl, The Phenomenological Theory of Linear Viscoelastic Behavior, Springer-Verlag, Berlin, 1989.
[16] F. Povolo, C.L. Matteo, Mater. Trans., JIM 33 (1992) 824.
[17] C.L. Matteo, Rheol. Acta 35 (1996) 308.
[18] S. Havriliak Jr., S. Negami, J. Polym. Sci. C 14 (1966) 99.
[19] S. Havriliak Jr., S. Negami, Polymer 8 (1967) 161.
[20] O.A. Lambri, in: J. Martinez-Mardones, D. Walgraef, C.H. Wörner (Eds.), Materials Instabilities, 2000, p. 249.
[21] Peak Fit, V. 4, Jandel Scientific Software, Germany, 1995.
[22] M. Suezawa, H. Kimura, Philos. Mag. 28 (1973) 901.
[23] I.A. Schwirtlich, H. Schultz, Philos. Mag. A 42 (1980) 601.
[24] R. Ziegler, H.E. Schaefer, in: International Conference on Vacancy and Interstitials in metals and alloys, Berlin, September 1986.
[25] O.A. Lambri, M. Massot, W. Riehemann, E.J. Lucioni, F. Plazaola, J.A. García, Phys. Status Solidi (a) 204 (2007) 1077.